Published in final edited form as:
Dev Biol. 2009 January 1; 325(1): 189–199. doi:10.1016/j.ydbio.2008.10.017.

dlx3b/4b are required for the formation of the preplacodal region and otic placode through local modulation of BMP activity

Robert Esterberg and **Andreas Fritz**
Department of Biology, Emory University, 1510 Clifton Rd., Atlanta, GA, 30322, USA

Abstract

The vertebrate inner ear arises from the otic placode, a transient thickening of ectodermal epithelium adjacent to neural crest domains in the presumptive head. During late gastrulation, cells fated to comprise the inner ear are part of a domain in cranial ectoderm that contain precursors of all sensory placodes, termed the preplacodal region (PPR). The combination of low levels of BMP activity coupled with high levels of FGF signaling are required to establish the PPR through induction of members of the *six/eya/dach*, *iro*, and *dlx* families of transcription factors. The zebrafish *dlx3b/4b* transcription factors are expressed at the neural plate border where they play partially redundant roles in the specification of the PPR, otic and olfactory placodes. We demonstrate that *dlx3b/4b* assist in establishing the PPR through the transcriptional regulation of the BMP antagonist *cv2*. Morpholino-mediated knockdown of Dlx3b/4b results in loss of *cv2* expression in the PPR and a transient increase in Bmp4 activity that lasts throughout early somitogenesis. Through the *cv2*-mediated inhibition of BMP activity, *dlx3b/4b* create an environment where FGF activity is favorable for PPR and otic marker expression. Our results provide insight into the mechanisms of PPR specification as well as the role of *dlx3b/4b* function in PPR and otic placode induction.

Keywords

dlx3b/4b; *cv2*; Bmp; Fgf; preplacodal region; otic placode

The interface between neural and non-neural ectoderm gives rise to several cell types, including neural crest, paired placodes and, in anamniotes, Rohon-Beard sensory neurons (Baker and Bronner-Fraser, 1997; Gans and Northcutt, 1983; Holland and Holland, 2001; Meulemans and Bronner-Fraser, 2004; Northcutt and Gans, 1983; Schlosser, 2006). The paired placodes, transient thickenings of ectodermal epithelium, arise lateral and adjacent to neural crest and Rohon-Beard domains in the presumptive head. During late gastrulation and early segmentation stages, placodal cells comprise a domain of cranial ectoderm that contains precursors of all sensory placodes (termed the preplacodal region, or PPR) (reviewed in Bailey and Streit, 2006; Ohyama et al., 2007; Riley, 2003; Schlosser, 2006). Evidence from studies in *Xenopus*, zebrafish, and chick suggest that the convergence of multiple activities of signaling molecules are required for the establishment of the PPR. A balance of FGF activity and antagonism of both BMP and WNT signaling are required to induce expression of members of the *Eyes absent* (*Eya*)/*Sine oculis* (*Six*)/*Dachshund* (*Dach*), *Iroquois* (*Iro*), and *Distalless*

Corresponding author: Andreas Fritz, Ph.D., Department of Biology, Emory University, 1510 Clifton Rd., Atlanta, GA, 30322, Phone: (404) 727-9012; Email: E-mail: afritz@emory.edu.

(*Dlx*) families of transcription factors during late gastrulation, which are the earliest markers of PPR fate (Ahrens and Schlosser, 2005; Brugmann et al., 2004; Glavic et al., 2004; Litsiou et al., 2005; Nguyen et al., 1998). In particular, modulation of BMP activity at the neural plate border is instrumental in the establishment of the PPR and also patterns adjacent Rohon-Beard and neural crest domains (Nguyen et al., 1998; Nguyen et al., 2000; Rossi et al., 2008; Tribulo et al., 2003).

In *Xenopus* and zebrafish, a BMP gradient model has been proposed in which BMP activity is high in ventral/lateral regions and progressively lower in more dorsal/medial regions during gastrulation. High levels of BMP activity are required to induce epidermis, low levels are required to specify neural plate, and intermediate levels are required to specify neural crest and Rohon-Beard domains (Aybar and Mayor, 2002; Nguyen et al., 1998; Nguyen et al., 2000; Tribulo et al., 2003). Although the PPR lies lateral to the domain of neural crest, evidence from *Xenopus*, zebrafish and chick suggests that BMP activity must be lower in the PPR than in adjacent neural crest and epidermal territories (Ahrens and Schlosser, 2005; Glavic et al., 2004; Litsiou et al., 2005). For example, implantation of Bmp4-containing beads near the PPR is sufficient to inhibit expression of the PPR marker *Six1* (Ahrens and Schlosser, 2005). Thus, it appears that establishment of the PPR requires lower levels of BMP activity than that required for neural crest and Rohon-Beard formation, contradictory to a simple gradient model.

While it is apparent that attenuation of BMP activity is critical in establishing the PPR, it is not yet clear how this attenuation is achieved. Tissue grafting experiments have revealed that potential BMP antagonists originate from tissues other than the PPR. Grafting of chicken head mesoderm onto extraembryonic ectoderm yields host tissue with PPR characteristics (Litsiou et al., 2005). Likewise, transplantation of neural ectoderm into domains of ventral ectoderm yields similar results in *Xenopus*, demonstrating the role these tisues have in creating an environment suitable for the formation of the PPR (Ahrens and Schlosser, 2005). However, the BMP antagonists involved in this process remain unidentified.

Members of the *Dlx* family of transcription factors are thought to play intrinsic roles in the formation of the PPR, although the mechanisms by which they do so are unclear. *Dlx* genes are required but not always sufficient for the expression of PPR markers from the *Eya/Six/Dach* families. For example, ectopic expression of *Six1* in *Xenopus* and chick can only be achieved in the presence of functional Dlx3 and Dlx5, respectively (Woda et al., 2003). In zebrafish, *dlx3b/4b* are initially expressed along the entire neural plate border, which includes the PPR, at the end of gastrulation. Expression becomes restricted to the otic and olfactory placodes during somitogenesis (Ekker et al., 1992; Feledy et al., 1999; Pera et al., 1999). Only rudimentary otic and olfactory placodes form when *dlx3b/4b* function is lost, and the resulting size of these sensory organs is significantly reduced (reviewed in Ohyama et al., 2007; reviewed in Riley, 2003). Induction of early otic and olfactory markers, such as *pax2a* and *eya1*, is severely compromised, suggesting that *dlx3b/4b* function early in the process of otic and olfactory induction. Thus, it has been suggested that *Dlx* genes may act as competence factors for placode induction (Hans et al., 2007; Hans et al., 2004).

In amniotes, *Dlx5* and *Dlx6* are expressed in a similar pattern to *dlx3b/4b* in zebrafish (Acampora et al., 1999; Yang et al., 1998). However, inactivation of *Dlx5/6* in mouse does not appear to affect induction of the otic or olfactory placodes, but rather their subsequent development (Merlo et al., 2002; Robledo and Lufkin, 2006; Robledo et al., 2002). The reason for the discrepancy in phenotypes between zebrafish and mouse embryos lacking these *Dlx* paralogues is currently unclear.

To better understand the role of *dlx3b/4b* during the establishment of the PPR and otic placodes, we examined signaling activities involved in PPR and otic placode induction. We have

identified that a BMP signaling modulator, Cv2, is critical for the formation of the PPR. The predominant function of this protein is as a BMP antagonist, although its proteolytic cleavage may allow Cv2 to act as an agonist of BMP activity (Rentzsch et al., 2006; Zhang et al., 2007; Zhang et al., 2008). We show that *cv2* lies transcriptionally downstream of *dlx3b/4b*, and that the full-length protein is required to modulate BMP activity to levels conducive for PPR formation. Morpholino-mediated knockdown of Dlx3b/4b results in loss of *cv2* expression in the PPR and a transient increase in Bmp4 activity that is first observed at the end of gastrulation. This is followed by a transient decrease in FGF activity that can be rescued when *cv2* or *fgf-receptor 1* (*fgfr1*) mRNA is supplied in Dlx3b/4b morphants. Ectopic expression of either *dlx3b* or *cv2* is sufficient to drive PPR marker expression. Conversely, loss of *cv2* has similar effects on PPR development as loss of *dlx3b/4b*, indicating that a significant aspect of *dlx3b/4b* function at the end of gastrulation is mediated through *cv2*. Our results suggest a model in which *dlx3b/4b*-mediated modulation of BMP signaling through *cv2* lies upstream of *Six/Eya/Dach* genes and FGF responsiveness in the specification of the PPR and induction of the otic placode. Furthermore, our findings provide a possible explanation for the difference in function of the *Dlx* genes between mouse and zebrafish.

Materials and Methods

Animals

Wild-type (AB) mutant zebrafish were obtained from the Zebrafish International Resource Center (Eugene, OR). Embryos were maintained at 28.5°C and staged using standard criteria (Kimmel et al., 1995). *Tg(hsp70l:dnBmpr-GFP)*^{w30} (*tBR*) transgenic zebrafish were obtained from the Kimelman lab (University of Washington, Seattle). This transgenic line contains a truncated Type I Bmp receptor containing GFP in place of the kinase domain under the control of a heat-shock promoter (Pyati et al., 2005). *tBR* embryos were heat shocked at 37°C for one hour at bud stage according to Pyati et al. (2005). They were then sorted according to GFP expression and raised at 28.5°C until fixation. Where appropriate, wild-type or control morpholino-injected embryos were heat-shocked at the same stage as controls.

In situ hybridization

The following probes were used: *bmp4* (Nikaido et al., 1997), *chordin* (Miller-Bertoglio et al., 1997), *cv2* (Rentzsch et al., 2006), *dlx3b* (Ekker et al., 1992), *erm* (Raible and Brand, 2001), *eya1* (Sahly et al., 1999), *fgfr1* (Scholpp et al., 2004), *fgfr2* (Poss et al., 2000), *fgfr3* (Sleptsova-Friedrich et al., 2001), *fgfr4* (Thisse et al., 1995), *pax2a* (Krauss et al., 1991), *six4.1* (Kobayashi et al., 2000), *spry4* (Fürthauer et al., 2001), and *tbx2b* (Dheen et al., 1999).

Real-time quantitative RT-PCR

RNA was isolated from three sets of 20 embryos of each experimental sample using the RNeasy kit (Qiagen). The SYBR Green I (Roche Applied Science) RNA amplification kit was used on the LightCycler according to the manufacturer's instructions and published protocols (Rajeevan et al., 2001). The primers used for each of the genes were: *bmp4* 5'-AGCCAACACCGTGAGAGGATTC -3' and 5'-TCTGCGGTGGATATGAGTTCGTC -3'; *fgfr1* 5'- GCGGCTCCCCAATGCTCTCAG -3' and 5'- ATCGCCTCGGCCATCATCACC -3'; *fgfr2* 5'- CACATCAACGGCGGCATAAAAACAT -3' and 5'-TCGGGATCTGATTGGGAAGTAAC -3'; *fgfr3* 5'- GTGGCGGGAGTCGGGGATACAG -3' and 5'- ATTGATGATGCGGAGGGCTTTCT -3'; *fgfr4* 5'-CAATCAGGGTCATAAGGCAGTTCA -3' and 5'- GCAGCGCCAGAGGGAACGAAC -3'; *ef1α* 5'- GTACTACTCTTCTTATGCCC -3' and 5'- GTACAGTTCCAATACCTCCA -3'. The different samples were standardized using EF-1α transcript levels as a reference. Each experimental run was also performed in triplicate. Transcript levels were compared by one-way ANOVA, followed by a two-tailed, equal variance *t*-test.

Morpholino injection

Morpholino injections against *bmp4* (Chocron et al., 2007), *chordin* (Nasevicius and Ekker, 2000), *cv2* (mo1 sequence was used; Rentzsch et al., 2006) and *dlx3b/4b* (Solomon and Fritz, 2002) have been previously characterized. The control morpholino sequence was 5'-CCTCTTACCTCAGTTACAATTTATA -3'. For interaction analyses, *chd* mo concentration was chosen that elicited a V1 ventralization phenotype, approximately 2.5ng (Kishimoto et al., 1997; Mullins et al., 1996). *dlx3b/4b* mo concentration was chosen that elicited a mild otic phenotype, approximately 5ng each.

mRNA synthesis

Capped mRNAs were transcribed using T7 and SP6 RNA polymerase in vitro transcription kits (mMESSAGE mMACHINE; Ambion). *fgfr1* cDNA was amplified using the following primers: 5'- TTTGATAATAATAATGAAGATGATGATGATAAT -3' and 5'-ATGACGGATGTATTTGAGTTTTGAGA-3'. It was then cloned into pCRII-TOPO, digested with *Spe*I and *Xho*I and ligated into pCS2+ digested with *Xba*I and *Xho*I. The vector was linearized with *Apa*I and mRNA was synthesized using SP6 polymerase. For rescue of the Dlx3b/4b morphant phenotype, approximately 15pg mRNA was co-injected into one- and two-cell embryos with *dlx3b/4b* MOs. *bmp2b, bmp4, dlx3b, cv2*, and *cv2-N* mRNA were synthesized and injected as previously described (Kishimoto et al., 1997; Rentzsch et al., 2006; Solomon and Fritz, 2002; Szeto and Kimelman, 2004).

Antibody staining

Labeling with PSMAD1/5/8 was as previously described (Rentzsch et al., 2006). The primary antibody was used at a dilution of 1:100 (anti-P SMAD1/5/8; Chemicon International). Secondary antibody was Alexa Fluor 594 goat anti-rabbit IgG at 1:500 (Molecular Probes).

Results

dlx3b/4b transiently regulate BMP activity

In *Xenopus* and chick, ectopic expression of BMP antagonists can induce ectopic PPR marker expression, while exposure to increased amounts of Bmp4 can ablate ectopic expression and reduce endogenous expression of the PPR markers *Six1/4* and *Eya2* (Ahrens and Schlosser, 2005; Brugmann et al., 2004; Litsiou et al., 2005). Furthermore, *Xenopus Dlx3* and chick *Dlx5* are both necessary and sufficient for *Six1* expression (McLarren et al., 2003; Woda et al., 2003), suggesting that *Dlx* genes lie upstream of *Eya/Six/Dach* members in the establishment of the PPR. Because of the inhibitory role of Bmp4 in PPR marker expression, we examined BMP activity in Dlx3b/4b morphants. Although we did not observe changes in *bmp4* expression prior to late gastrulation, the domain of *bmp4* expression in prechordal mesoderm and tailbud was expanded in Dlx3b/4b morphants beginning at bud stage (Figure 1C,D). By mid-somitogenesis expression levels returned to those seen in embryos injected with control morpholino (Figure 1G,H). To quantify this increase in Bmp4 activity, we performed quantitative RT-PCR on mRNA extracted from bud stage Dlx3b/4b morphants. *bmp4* transcripts were detected to be elevated by approximately 40% in bud stage Dlx3b/4b morphants ($p<0.005$; Supplemental Figure 1). We also examined the expression of *bmp2b*, which is expressed in a pattern similar to *bmp4* at the end of gastrulation, and which has been shown to be misregulated in *dlx3b/4b* morphant embryos (Kaji and Artinger, 2004). Consistent with previous observations (Kaji and Artinger, 2004), *bmp2b* transcript levels were reduced by approximately 15% in Dlx3b/4b morphants (data not shown).

To determine the effects of *bmp4* misregulation in Dlx3b/4b morphants, we labeled embryos with antibodies against phosphorylated (P)SMAD1/5/8, which is activated in response to BMP

signaling (Yamamoto and Oelgeschlager, 2004). We observed an increase in PSMAD1/5/8 localization in the anterior neural plate of Dlx3b/4b morphants (Figure 1E,F), indicating that these cells have received and are responding to BMP signaling.

This transient misregulation of Bmp4 activity results in morphological dorsoventral (DV) patterning defects; Dlx3b/4b morphants exhibit an increase in intermediate cell mass of the tail similar to the mildest class of ventralization mutants (Figure 2B; Kishimoto et al., 1997; Mullins et al., 1996). Because the ventralization phenotype of Dlx3b/4b morphants is mild, we wished to demonstrate that loss of Dlx3b/4b can increase the severity of ventralization in a sensitized background. We determined an amount of *chordin* (*chd*) morpholino that was sufficient to phenocopy the V1 ventralization phenotype and injected it in combination with *dlx3b/4b* morpholinos. In Chd/Dlx3b/4b triple morphants, the ventralization phenotype was compounded such that embryos resembled the V2 class of ventralization mutants, with a greater expanse in the tail than seen in Chd or Dlx3b/4b morphants alone (Figure 2B-D).

To further confirm that BMP activity is increased in Dlx3b/4b morphants we examined *chd* expression. BMP antagonists expressed on the dorsal side of the embryo, such as *chd*, are negatively regulated by BMP signaling (reviewed in Kimelman and Szeto, 2006; Yamamoto and Oelgeschlager, 2004). *chd* expression was reduced in the anterior neural plate and paraxial mesoderm of bud stage and 6-somite Dlx3b/4b morphants (Supplemental Figure 2B,F,J), consistent with observed elevated BMP levels.

dlx3b/4b mediate BMP signaling through *cv2*

Cv2 plays a role throughout embryogenesis predominantly as an antagonist of Bmp4 (Ambrosio et al., 2008; Rentzsch et al., 2006; Serpe et al., 2008; Zhang et al., 2008). During late gastrulation, *cv2* is expressed in a pattern around the neural plate (Figure 3C-F; Rentzsch et al., 2006) resembling that of *dlx3b/4b*. Our analysis suggests that this pattern of expression spatially overlaps with *dlx3b* in preplacodal ectoderm (Figure 3A,B), rather than being localized to the underlying mesendoderm as initially suggested (Rentzsch et al., 2006). Following early somitogenesis, *cv2* and *dlx3b/4b* are expressed in the otic placode and pharyngeal arches, raising the possibility that *cv2* lies transcriptionally downstream of Dlx3b/4b (Figure 3G-J; Ekker et al., 1992; Rentzsch et al., 2006). Morpholino-mediated knockdown of Dlx3b/4b resulted in a loss of *cv2* expression from the PPR during late gastrulation, as well as in the otic placodes and pharyngeal arches during somitogenesis (Figure 3E-J). Importantly, *cv2* expression was not lost from ventral tissues before the onset of *dlx3b/4b* expression or tail mesoderm during somitogenesis, where its expression does not overlap with *dlx3b/4b* (data not shown; Figure 3C,D,G,H; Rentzsch et al., 2006).

Because loss of Dlx3b/4b increases BMP activity, we wished to determine the effects of overexpressing *dlx3b*. To do so, we injected *dlx3b* mRNA into one- and two-cell embryos. *bmp4* expression and PSMAD1/5/8 staining were reduced in embryos ectopically expressing *dlx3b* mRNA (Figure 4A-D). We also observed expansion of the hindbrain marker *krox20* in these embryos (Figure 4E,F), consistent with a dorsalization phenotype (Kishimoto et al., 1997; Mullins et al., 1996).

Because *cv2* expression is lost from *dlx3b/4b*-expressing tissues in Dlx3b/4b morphants, we wished to explore whether elevated BMP activity observed in these morphants was due to *cv2*. To demonstrate that *dlx3b* activates *cv2* expression cell-autonomously, the *dlx3b* ORF was cloned into pCS2+ and injected into 1-cell embryos. Typically, injection of plasmid DNA leads to mosaic distribution of the DNA in later stage embryos. In these embryos, *cv2* was co-expressed in the same cells ectopically expressing *dlx3b* (Figure 4G,H).

Furthermore, embryos ectopically expressing *dlx3b* or *cv2* mRNA were moderately (59%; 67/113 and 34; 49/146, respectively) or severely (41%; 46/113 and 24%; 35/146, respectively) dorsalized (Figure 4I-K,M,N), resembling C3 and C4 classes of dorsalization, respectively (Kishimoto et al., 1997; Mullins et al., 1996). Knockdown of Cv2 was able to rescue the dorsalization phenotype seen in embryos ectopically expressing *dlx3b* mRNA (Figure 4L).

Similarly, *chd* expression in embryos ectopically expressing a dominant negative form of *cv2* mRNA (*cv2-N*; Rentzsch et al., 2006) resembled that of Dlx3b/4b morphants (Supplemental Figure 2D,H,L). Co-injection of *cv2* mRNA with *dlx3b/4b* morpholinos was sufficient to rescue *chd* expression (Supplemental Figure 2C,G,K), demonstrating that the modulation of BMP activity by *dlx3b/4b* depends at least in part on *cv2*.

dlx3b/4b-mediated expression of *cv2* is necessary for PPR marker expression

Because we observed an increase in BMP activity and a loss of *cv2* expression from the PPR of Dlx3b/4b morphants, we wished to determine how disruption of Dlx3b/4b or Cv2 affects PPR formation. BMP activity, particularly Bmp4, inhibits the expression of PPR markers from the Six/Eya/Dach transcriptional network (reviewed in Bailey and Streit, 2006; Brugmann and Moody, 2005; Schlosser, 2006). Expression of the PPR markers *eya1* and *six4.1* is lost from the PPR of bud stage Dlx3b/4b and Cv2 morphant embryos (Figure 5A-C,F-H,). PPR marker expression was restored either when Bmp4 was knocked down or when *cv2* mRNA was ectopically expressed in Dlx3b/4b morphants (Figure 5D,E,I,J). Although the width of the PPR was not significantly altered in these embryos, we did observe ectopic expression of both *eya1* and *six4.1* within the neural plate.

Studies in *Xenopus* have demonstrated that *Dlx3* is required to position the PPR. Inhibition of endogenous Dlx activity expands the neural plate at the expense of the PPR (Woda et al., 2003). To determine whether *dlx3b* was sufficient to induce ectopic PPR marker expression, we injected the pcs2⁜*dlx3b* DNA construct into one-cell embryos. Under these conditions ectopic *dlx3b* was sufficient to induce ectopic expression of both *eya1* and *six4.1* (Figure 5K, data not shown). Because we were able to rescue the PPR phenotype of Dlx3b/4b morphants by supplying *cv2* mRNA, we wished to determine the effects of ectopic *cv2* on PPR formation, independent of *dlx3b*. Injection of pcs2⁜*cv2* was sufficient to drive ectopic *eya1* or *six4.1* expression (Figure 5L, data not shown). Ectopic PPR marker expression was not observed when pcs2⁜*dlx3b* was co-injected with *cv2* morpholino (data not shown), suggesting that the PPR inducing properties of *dlx3b* require *cv2*.

A small number of cells that expressed either ectopic *dlx3b* or *cv2* did not co-express *eya1* or *six4.1*. Although full length Cv2 acts as a BMP antagonist, it is subject to proteolytic cleavage that renders it an agonist of BMP activity (Rentzsch et al., 2006; Zhang et al., 2008). We reasoned that the processing of Cv2 into a BMP agonist was responsible for the cells not expressing ectopic *eya1* or *six4.1*. As such, we injected a DNA construct containing an uncleavable form of the *cv2* ORF, in which the cleavage site of Cv2 is mutated (*cv2-CM*; Rentzsch et al., 2006), into one-cell embryos and assayed ectopic PPR marker expression (Rentzsch et al., 2006). In these embryos, all cells ectopically expressing *cv2-CM* co-expressed *eya1* and *six4.1* (Figure 5M, data not shown). These results suggest that Dlx3b/4b establish the PPR through transcriptional regulation of *cv2*. Furthermore, induction of PPR marker expression requires low levels of BMP activity, particularly Bmp4. This is mediated through the uncleaved form of Cv2, suggesting that in this context *cv2* acts as a BMP antagonist.

Cv2 antagonism of BMP activity promotes FGF activity

Establishment of the PPR requires not only the attenuation of BMP activity but FGF activity as well (Ahrens and Schlosser, 2005; Bailey and Streit, 2006; Brugmann and Moody, 2005;

Litsiou et al., 2005; Schlosser, 2006). Since ectopic expression of either *dlx3b* or *cv2* induced expression of both *eya1* and *six4.1*, we wished to examine the effects of *dlx3b* and *cv2* on FGF activity. The expression of genes induced by FGF activity, including *erm* and *spry4* (Fürthauer et al., 2001; Raible and Brand, 2001), was observed in cells ectopically expressing *dlx3b* or *cv2* (Figure 6A,B,D,E). Ectopic *fgf receptor1* (*fgfr1*) expression was also detected in cells ectopically expressing *dlx3b* or *cv2* (Figure 6C,E). As with PPR marker expression, some cells expressing ectopic *cv2* did not express markers indicative of FGF responsiveness. We were able to drive all cells expressing the uncleavable form of *cv2* to express markers indicative of FGF competence (Figure 6G-I).

In addition to the role of FGF signaling in PPR formation, numerous studies have established that Fgf3/8 signaling from the mesendoderm and hindbrain are required for otic placode induction in zebrafish (Leger and Brand, 2002; Liu et al., 2003; Riley, 2003; Riley and Phillips, 2003; Solomon et al., 2004). The expression of these FGF ligands is unaffected by loss of Dlx3b/4b (Liu et al., 2003; Solomon et al., 2004). Nonetheless, Dlx3b/4b are required for the proper expression of the FGF target gene *pax2a* in otic placode induction (Leger and Brand, 2002; Phillips et al., 2001). Because our results suggested that Dlx3b/4b and Cv2 may affect competence to respond to FGF activity, we examined the expression of *erm* and the three *fgf receptors* (*fgfr1-3*) expressed in the otic placode (Poss et al., 2000; Scholpp et al., 2004; Sleptsova-Friedrich et al., 2001; Thisse et al., 1995). *erm* expression was lost from the hindbrain and otic placode of Dlx3b/4b morphants at the 6-somite stage (Figure 7A,B). We observed decreases in *fgfr1-3* expression in the otic placode as well as in the hindbrain of Dlx3b/4b morphants (Figure 7E,H,K). *fgfr1* transcript, which is localized in rhombomere 3 of the hindbrain, otic placode, and MHB, was lost from both rhombomere 3 and the otic placodes of Dlx3b/4b morphants (Figure 7E). Similarly, *fgfr2* expression was lost from rhombomeres 4 and 6 as well as the otic placode in Dlx3b/4b morphants (Figure 7H). *fgfr3* expression was lost from the hindbrain and otic placode in Dlx3b/4b morphants (Figure 7K). Quantification of *fgfr* transcript levels in Dlx3b/4b morphants revealed that transcripts were reduced by approximately 30% compared to embryos injected with control morpholinos ($p<0.005$; Supplemental Figure 1). The decrease in *fgfr* expression in Dlx3b/4b morphants is transient; we did not observe a change in *erm* or *fgfr* expression until early somitogenesis, after the increase in *bmp4* expression (Supplemental Figure 3). Like the increase in *bmp4* expression, *erm* and *fgfr* expression returned to levels comparable to controls by mid-somitogenesis (Supplemental Figure 4).

To determine whether the addition of *cv2* could rescue the decrease in FGF activity seen in Dlx3b/4b morphants, we co-injected *cv2* mRNA with *dlx3b/4b* morpholinos into one- and two-cell embryos. Ectopic *cv2* expression was sufficient to restore *erm* expression in the otic placode and hindbrain of Dlx3b/4b morphants (Figure 7C). Likewise, *fgfr1-3* expression returned to otic and hindbrain domains in Dlx3b/4b morphants (Figure 7F,I,L). Taken together, these results suggest that through their regulation of the BMP antagonist *cv2*, Dlx3b/4b indirectly promote competence to respond to FGF signaling.

Inhibition of BMP activity can rescue the otic phenotype of Dlx3b/4b morphants

Previous studies have shown that *pax2a* expression is delayed in the otic placode of Dlx3b/4b morphants until mid-somitogenesis stages (Liu et al., 2003; Solomon et al., 2004), which corresponds with the transient reduction in *fgfr* expression we observe in these morphants. As we observed rescue of *erm* expression when *cv2* mRNA was co-injected with *dlx3b/4b* morpholinos, we wished to determine if ectopic *cv2* mRNA was sufficient to rescue *pax2a* expression in Dlx3b/4b morphants. While we observed variability in the width of the midbrain-hindbrain boundary (MHB) and optic stalk of Cv2 morphants consistent with mild DV patterning defects (Rentzsch et al., 2006), *pax2a* expression was consistently absent from the

otic placode (Figure 8B-D). Injection of *cv2* mRNA at levels that did not significantly affect DV patterning was sufficient to rescue *pax2a* expression in the otic placode (Figure 8E).

Despite its inhibition of PPR induction, the role of BMP activity in otic placode development has not been examined (reviewed in Ohyama et al., 2007; Riley, 2003). To examine the effects of elevated BMP activity levels on otic development, we inactivated Dlx3b/4b and Chd in concert. In Dlx3b/4b/Chd triple morphants the expression of *eya1*, *pax2a*, and *tbx2b* was lost from the otic vesicle yet maintained in surrounding tissues (Figure 2E-M). Therefore, we determined further how manipulation of Cv2 and BMP activity affects otic development in a Dlx3b/4b morphant background. Dlx3b/4b morphants develop an otic vesicle that is reduced in size and lacks otoliths (Figure 9A,B) (Liu et al., 2003; Solomon and Fritz, 2002). Although slightly larger, the otic vesicle of Cv2 morphants resembled that of Dlx3b/4b morphants (Figure 9C). The otic phenotype of Cv2/Dlx3b/4b triple morphants was no more severe than Dlx3b/4b morphants (Figure 9D). Furthermore, the otic phenotype of Dlx3b/4b morphants was rescued when *cv2* mRNA was co-injected with *dlx3b/4b* morpholinos (Figure 9E,F).

To demonstrate that the otic phenotype of Dlx3b/4b morphants is due to the loss of BMP antagonizing activity of Cv2, we took advantage of a transgenic zebrafish line carrying a truncated form of a type I BMP receptor under the control of a heatshock promoter (abbreviated *tBR*; Pyati et al., 2005). In order to attenuate BMP signaling over the stages at which we observed increased BMP activity in Dlx3b/4b morphants, we heat-shocked *tBR* embryos at bud stage. Attenuating BMP activity in Dlx3b/4b morphants was sufficient to rescue the otic phenotype of Dlx3b/4b morphants Figure 9G,H). A similar rescue was observed when Bmp4 was knocked down in concert with Dlx3b/4b Figure 9I,J). This suggests that elevated BMP activity inhibits otic placode induction, and that a major role of Dlx3b/4b is to modulate BMP activity levels in the otic placode, primarily through regulation of *cv2* expression.

Because we observed a depression of FGF activity in Dlx3b/4b morphant embryos, we tested whether the Dlx3b/4b morphant phenotype could be rescued by supplying *fgfr* mRNA to Dlx3b/4b morphants. To do so, we overexpressed *fgfr1*, the Fgf receptor responsible for mediating Fgf8 signaling (Scholpp et al., 2004). Injection of *fgfr1* mRNA was also able to partially rescue the Dlx3b/4b morphant phenotype (81%; 104/129); the otic vesicle in these embryos was larger and contained one otolith (Figure 9K,L). Taken together, these results suggest that BMP activity in the otic placode inhibits the ability of preotic cells to respond to FGF signaling, and that this inhibition occurs at the level of *fgfr* expression.

Discussion

Numerous studies have shown that placodal precursor cells are derived from a molecularly and embryologically distinct domain, the PPR (Bhattacharyya et al., 2004; David et al., 2001; Ekker et al., 1992; Kobayashi et al., 2000; Kozlowski et al., 1997; Sahly et al., 1999; Streit, 2002; Whitlock and Westerfield, 2000). PPR formation is a complex process that requires the interplay of several signaling pathways, notably high levels of FGF and low levels of BMP activity (Ahrens and Schlosser, 2005; Brugmann et al., 2004; Glavic et al., 2004; Litsiou et al., 2005). To understand the development of sensory placodes, it is crucial to determine how the PPR is generated.

Members of the *Dlx* gene family are expressed in the PPR, raising the possibility that they mediate signaling events to levels conducive for further sensory placode development. In zebrafish *dlx3/4b* are required for at least otic and olfactory placode development, and in *Xenopus Dlx3* is required for the induction of *Six1* in the PPR (Solomon and Fritz, 2002; Woda et al., 2003), suggesting that *Dlx* genes play a central role in placodal competence (Hans et al.,

2007; Hans et al., 2004). In this context, we have reexamined the role of *dlx3b/4b* in both the establishment of the PPR and otic placode induction.

Modulation of BMP activity by *dlx3b/4b* at the neural plate border

Here we show that *dlx3b/4b* are both necessary and sufficient for the expression of *cv2* in the PPR and developing otic placode. Loss of Dlx3b/4b function leads to a transient increase in Bmp4 activity at the end of gastrulation and early somite stages. Introduction of *cv2* mRNA or inhibition of Bmp4 or total BMP activity can rescue the PPR and otic phenotypes observed in Dlx3b/4b morphants, demonstrating that Dlx3b/4b mediate BMP activity in the PPR. In the context of PPR specification and otic induction, Dlx3b/4b appear to act as permissive factors, allowing the expression of *Eya/Six/Dach* gene members in the PPR and *pax2a* in the otic placode without any direct transcriptional requirement.

In addition to their role in PPR formation, *dlx3b/4b* likely have other functions at the neural plate border. Our analysis shows that increased BMP signaling is not limited to *dlx3b/4b*-expressing cells as Dlx3b/4b morphant embryos are mildly ventralized in the tail region. Furthermore, studies by Artinger and colleagues have demonstrated that *Dlx*-expressing cells at the neural plate border in *Xenpus* and zebrafish affect neighboring cells in the lateral neural plate domain (Kaji and Artinger, 2004; Woda et al., 2003). The secretion of Cv2 from the PPR posits a likely mechanism of how *Dlx* genes can autonomously establish the PPR while exerting non-autonomous influence over the adjacent neural crest/Rohon-Beard domain. Recent studies in *Drosophila* and *Xenopus* have shown that Cv2 preferentially binds Bmp4 (and Dpp in *Drosohpila*), and that its pro- or anti- BMP effects occur in a dose-dependent manner (Ambrosio et al., 2008; Serpe et al., 2008), such that high Cv2 levels inhibit Bmp4 ligand-receptor interactions, while low Cv2 levels stabilize them. Furthermore, due to interactions of Cv2 with heparin sulfate proteoglycans, these activities occur over a very short distance from the secreted cell (Rentzsch et al., 2006; Serpe et al., 2008), potentially explaining why ectopic PPR marker expression is not observed at any distance from *cv2*-expressing cells. This evidence supports our model in which high levels of Cv2 secreted by *dlx3b/4b*-expressing cells establishes the presumptive PPR by inhibiting Bmp4 signaling, and may explain how Cv2 enhances the Bmp4 requirements in neural crest and Rohon-Beard cells (Rossi et al., 2008). However, due to the recently revealed complexities that govern Cv2 function in BMP modulation (Ambrosio et al., 2008; Bier, 2008; Serpe et al., 2008; Zhang et al., 2008), this latter point remains to be investigated.

Integration of BMP and FGF signaling in PPR and placode formation

In both *Xenopus* and chick, FGF activity is required but not sufficient for the establishment of preplacodal territory (reviewed in Bailey and Streit, 2006; Schlosser, 2006). The combination of elevated levels of FGF activity and low levels of BMP activity, however, does appear to be able to induce the full range of PPR markers. *Six4*, which cannot be induced with ectopic Fgf8 activity alone, can be induced when BMP activity is inhibited in the presence of ectopic Fgf8 (Litsiou et al., 2005). Similarly in *Xenopus*, *Fgf8* can induce *Six1* expression only in the presence of the BMP antagonist *Noggin* (Ahrens and Schlosser, 2005). Together, these studies show that induction of the PPR requires a precise balance of high FGF activity and low BMP activity that is normally found at the border of the neural plate.

Despite these studies, it has remained unclear why PPR formation or otic placode induction require attenuation of BMP signaling. Although it is possible that BMP signaling is detrimental to the formation of these tissues per se, our evidence suggests that excessive BMP activity interferes with FGF signaling. Cells ectopically expressing *dlx3b* or *cv2* co-express markers indicative of PPR formation. Many of these cells also express *fgfr1* and the FGF feedback regulators *erm* and *spry4*, demonstrating Dlx3b/4b and Cv2 confer competence to respond to

FGF signaling. This appears to be through the BMP antagonizing activity of Cv2, as all cells ectopically expressing *cv2-CM* co-express *fgfr1*, *erm* and *spry4*. BMP signaling has similar effects in otic placode induction, where *fgfr1-3* expression is reduced in the otic placode and hindbrain of Dlx3b/4b morphants. Interestingly, we were able to significantly rescue both the PPR (data not shown) and otic vesicle defects seen in Dlx3b/4b morphants by overexpressing *fgfr1*. *fgfr1* has previously been shown to mediate Fgf8 signaling, a key component of otic placode induction (Leger and Brand, 2002; Phillips et al., 2001; Riley, 2003; Scholpp et al., 2004).

Interactions between BMP and FGF signaling pathways have been previously demonstrated. FGF signaling has been shown to interfere with BMP signaling by phosphorylation of the linker region of SMAD1 (Pera et al., 2003). Conversely, in murine limb bud development, BMP activity inhibits FGF signaling by downregulating *Fgf4* expression in the apical ectodermal ridge (Ganan et al., 1996; Pizette and Niswander, 1999; Zuniga et al., 1999). Our data suggest that in the context of PPR and otic placode induction, BMP activity leads to a downregulation of *fgfr* expression. This effect may be mediated by BMP targets such as the *vent/vox* transcriptional repressors (Imai et al., 2001; Melby et al., 2000; Shimizu et al., 2002); however, this remains to be elucidated. Thus, we propose that the balance of FGF and BMP activities at the neural plate border is established by in part by Dlx3b/4b through the transcriptional regulation of *cv2*. Our data suggest that Cv2 acts in its uncleaved, antagonistic form, and *dlx3/4b* acts to locally establish an environment of low BMP activity. Through the inhibition of BMP activity, Cv2 establishes a region favorable for FGF activity. While it has been suggested that BMP antagonists secreted from underlying mesendoderm act to regulate PPR fate (Litsiou et al., 2005), Cv2 is the first identified BMP antagonist expressed in the PPR itself that is required for the establishment of this tissue.

Although low BMP activity levels are critical for PPR formation at the end of gastrulation, the initial establishment of *dlx3b/4b* expression requires BMP signaling. Fate-mapping studies have shown that cells that will become the PPR originate from regions of the gastrula that are initially exposed to higher levels of BMP activity than those cells that will give rise to neural plate (Kozlowski et al., 1997). These differences in BMP exposure of presumptive PPR and neural ectoderm are reflected by expression of *Dlx*, *Foxi*, and *Msx* family members within presumptive PPR (Feledy et al., 1999; Luo et al., 2001; Matsuo-Takasaki et al., 2005; Nguyen et al., 1998; Pera et al., 1999; Phillips et al., 2006; Suzuki et al., 1997). BMP signaling directly regulates murine *Dlx3* expression through SMAD1 (Park and Morasso, 2002). Similarly, it has been demonstrated that *Dlx3/5/6* expression around chick and *Xenopus* neural plate are increased in response to elevated BMP activity levels (Feledy et al., 1999; Luo et al., 2001; Pera et al., 1999). In zebrafish *swirl* (*bmp2b*), *snailhouse* (*bmp7*), or *somitabun* (*smad5*) mutants, *dlx3b* is not expressed in the PPR or otic placode (data not shown; Nguyen et al., 1998). Thus, formation of the PPR first requires BMP signaling during early gastrulation to establish a domain of *Dlx* expression, which subsequently antagonizes BMP activity to levels favorable for induction of the PPR.

Dlx and Cv2: evolutionary implications for PPR establishment

In chick and mouse, *Cv2* is expressed in premigratory NC (Coffinier et al., 2002; Coles et al., 2004), a tissue that requires intermediate levels of BMP activity, while *cv2* expression in zebrafish overlaps with *dlx3b* in preplacodal ectoderm, a tissue that requires low levels of BMP activity (reviewed in Aybar and Mayor, 2002; Bailey and Streit, 2006; Schlosser, 2006). Furthermore, *Cv2* appears to act as an agonist of BMP signaling in chick NC development (Coles et al., 2004). Although *Cv2* expression in chick has not been determined at the relevant stages, it is difficult to reconcile the known *Cv2* expression and function in chick with our results in PPR formation. In mouse, *Cv2* does not appear to be expressed in the PPR at the

onset of somite stages (Coffinier et al., 2002). While *Cv2* expression needs to be more thoroughly examined in amniotes, it is clear that *Cv2* expression patterns have diverged between amniotes and zebrafish as there is no expression in zebrafish neural crest.

In amniotes, the *Dlx5/6* genes are expressed in a similar manner to zebrafish *dlx3b/4b* (Ekker et al., 1992; Pera et al., 1999; Yang et al., 1998). In chick, *Dlx5* misexpression leads to upregulation of *Six4* (McLarren et al., 2003), consistent with our observations in zebrafish. However, while the role of *Dlx5/6* in PPR formation has not been examined in detail in chick or mouse, knock-out of mouse *Dlx5/6* does not appear to affect the induction of the otic placode (Acampora et al., 1999; Merlo et al., 2002; Robledo and Lufkin, 2006; Robledo et al., 2002). Instead, mutant mice develop later defects in inner ear morphology. The role of the zebrafish *dlx3b/4b* genes in PPR establishment appears to remain conserved between *Xenopus* and zebrafish. While the *Xenopus Cv2* gene has been identified, its expression has not yet been analyzed (Coles et al., 2004; Moser et al., 2003). However, as discussed above, *Xenopus Dlx3* is required for expression of PPR markers in transplantation experiments, and Dlx3 in *Xenopus* appears to have similar effects on the lateral neural plate as seen in zebrafish (Kaji and Artinger, 2004; Woda et al., 2003). Therefore, it is likely that at least in fish and amphibians the role of these genes is similar.

Based on our analysis, we suggest that the discrepancy in the early role of the *Dlx* genes between mouse and zebrafish in PPR establishment and placode induction might be due to differences in *Cv2* expression. Thus, the *Dlx5/6* genes are unlikely to play a role in modulation of BMP signaling and establishment of the PPR and seem to be principally involved in later aspects of placode development. Importantly, even though the precise molecular mechanism of PPR induction may show species specific differences, the overall requirements for high levels of FGF activity and attenuated BMP activity appear to be the same in chick, amphibians, and fish (Ahrens and Schlosser, 2005; Brugmann et al., 2004; Glavic et al., 2004; Litsiou et al., 2005). Evidence from tissue culture in chick supports a model whereby BMP antagonists secreted from mesoderm underlying the PPR are required to position the PPR (Litsiou et al., 2005), although specific signaling antagonists that act to position the PPR have not yet been identified *in vivo* in chick or mouse. While our data do not exclude a role of the underlying mesendoderm in fish, we show that a key component in the attenuation of BMP signaling, *cv2*, is indeed expressed in the PPR itself.

Supplementary Material

Refer to Web version on PubMed Central for supplementary material.

Acknowledgements

We would like to thank P. Chen for comments and criticisms on the manuscript, D. Kimelman and U. Pyati for the *Tg(hsp70l:dnBmpr-GFP)*^{w30} zebrafish line, M. Esterberg for assistance with statistics. This work was supported by an NIH grant to A.F. (DC004701).

References

Acampora D, Merlo GR, Paleari L, Zerega B, Postiglione MP, Mantero S, Bober E, Barbieri O, Simeone A, Levi G. Craniofacial, vestibular and bone defects in mice lacking the Distal-less-related gene Dlx5. Development 1999;126:3795–809. [PubMed: 10433909]

Ahrens K, Schlosser G. Tissues and signals involved in the induction of placodal Six1 expression in Xenopus laevis. Dev Biol 2005;288:40–59. [PubMed: 16271713]

Ambrosio AL, Taelman VF, Lee HX, Metzinger CA, Coffinier C, De Robertis EM. Crossveinless-2 Is a BMP feedback inhibitor that binds Chordin/BMP to regulate Xenopus embryonic patterning. Dev Cell 2008;15:248–60. [PubMed: 18694564]

Aybar MJ, Mayor R. Early induction of neural crest cells: lessons learned from frog, fish and chick. Curr Opin Genet Dev 2002;12:452–8. [PubMed: 12100892]

Bailey AP, Streit A. Sensory organs: making and breaking the pre-placodal region. Curr Top Dev Biol 2006;72:167–204. [PubMed: 16564335]

Baker CV, Bronner-Fraser M. The origins of the neural crest. Part I: embryonic induction. Mech Dev 1997;69:3–11. [PubMed: 9486527]

Bhattacharyya S, Bailey AP, Bronner-Fraser M, Streit A. Segregation of lens and olfactory precursors from a common territory: cell sorting and reciprocity of Dlx5 and Pax6 expression. Dev Biol 2004;271:403–14. [PubMed: 15223343]

Bier E. Intriguing extracellular regulation of BMP signaling. Dev Cell 2008;15:176–7. [PubMed: 18694555]

Brugmann SA, Moody SA. Induction and specification of the vertebrate ectodermal placodes: precursors of the cranial sensory organs. Biol Cell 2005;97:303–19. [PubMed: 15836430]

Brugmann SA, Pandur PD, Kenyon KL, Pignoni F, Moody SA. Six1 promotes a placodal fate within the lateral neurogenic ectoderm by functioning as both a transcriptional activator and repressor. Development 2004;131:5871–81. [PubMed: 15525662]

Chocron S, Verhoeven MC, Rentzsch F, Hammerschmidt M, Bakkers J. Zebrafish Bmp4 regulates left-right asymmetry at two distinct developmental time points. Dev Biol 2007;305:577–88. [PubMed: 17395172]

Coffinier C, Ketpura N, Tran U, Geissert D, De Robertis EM. Mouse Crossveinless-2 is the vertebrate homolog of a Drosophila extracellular regulator of BMP signaling. Mech Dev 2002;119(Suppl 1):S179–84. [PubMed: 14516682]

Coles E, Christiansen J, Economou A, Bronner-Fraser M, Wilkinson DG. A vertebrate crossveinless 2 homologue modulates BMP activity and neural crest cell migration. Development 2004;131:5309–17. [PubMed: 15456729]

David R, Ahrens K, Wedlich D, Schlosser G. Xenopus Eya1 demarcates all neurogenic placodes as well as migrating hypaxial muscle precursors. Mech Dev 2001;103:189–92. [PubMed: 11335132]

Dheen T, Sleptsova-Friedrich I, Xu Y, Clark M, Lehrach H, Gong Z, Korzh V. Zebrafish tbx-c functions during formation of midline structures. Development 1999;126:2703–13. [PubMed: 10331981]

Ekker M, Akimenko MA, Bremiller R, Westerfield M. Regional expression of three homeobox transcripts in the inner ear of zebrafish embryos. Neuron 1992;9:27–35. [PubMed: 1352984]

Feledy JA, Morasso MI, Jang SI, Sargent TD. Transcriptional activation by the homeodomain protein distal-less 3. Nucleic Acids Res 1999;27:764–70. [PubMed: 9889271]

Fürthauer M, Reifers F, Brand M, Thisse B, Thisse C. sprouty4 acts in vivo as a feedback-induced antagonist of FGF signaling in zebrafish. Development 2001;128:2175–86. [PubMed: 11493538]

Ganan Y, Macias D, Duterque-Coquillaud M, Ros MA, Hurle JM. Role of TGF beta s and BMPs as signals controlling the position of the digits and the areas of interdigital cell death in the developing chick limb autopod. Development 1996;122:2349–57. [PubMed: 8756280]

Gans C, Northcutt RG. Neural Crest and the Origin of Vertebrates: A New Head. Science 1983;220:268–273. [PubMed: 17732898]

Glavic A, Maris Honore S, Gloria Feijoo C, Bastidas F, Allende ML, Mayor R. Role of BMP signaling and the homeoprotein Iroquois in the specification of the cranial placodal field. Dev Biol 2004;272:89–103. [PubMed: 15242793]

Hans S, Christison J, Liu D, Westerfield M. Fgf-dependent otic induction requires competence provided by Foxi1 and Dlx3b. BMC Dev Biol 2007;7:5. [PubMed: 17239227]

Hans S, Liu D, Westerfield M. Pax8 and Pax2a function synergistically in otic specification, downstream of the Foxi1 and Dlx3b transcription factors. Development 2004;131:5091–102. [PubMed: 15459102]

Holland LZ, Holland ND. Evolution of neural crest and placodes: amphioxus as a model for the ancestral vertebrate? J Anat 2001;199:85–98. [PubMed: 11523831]

Imai Y, Gates MA, Melby AE, Kimelman D, Schier AF, Talbot WS. The homeobox genes vox and vent are redundant repressors of dorsal fates in zebrafish. Development 2001;128:2407–20. [PubMed: 11493559]

Kaji T, Artinger KB. dlx3b and dlx4b function in the development of Rohon-Beard sensory neurons and trigeminal placode in the zebrafish neurula. Dev Biol 2004;276:523–40. [PubMed: 15581883]

Kimelman D, Szeto DP. Chordin cleavage is sizzling. Nat Cell Biol 2006;8:305–7. [PubMed: 16607266]

Kimmel CB, Ballard WW, Kimmel SR, Ullmann B, Schilling TF. Stages of embryonic development of the zebrafish. Dev Dyn 1995;203:253–310. [PubMed: 8589427]

Kishimoto Y, Lee KH, Zon L, Hammerschmidt M, Schulte-Merker S. The molecular nature of zebrafish swirl: BMP2 function is essential during early dorsoventral patterning. Development 1997;124:4457–66. [PubMed: 9409664]

Kobayashi M, Osanai H, Kawakami K, Yamamoto M. Expression of three zebrafish Six4 genes in the cranial sensory placodes and the developing somites. Mech Dev 2000;98:151–5. [PubMed: 11044620]

Kozlowski DJ, Murakami T, Ho RK, Weinberg ES. Regional cell movement and tissue patterning in the zebrafish embryo revealed by fate mapping with caged fluorescein. Biochem Cell Biol 1997;75:551–62. [PubMed: 9551179]

Krauss S, Johansen T, Korzh V, Fjose A. Expression of the zebrafish paired box gene pax[zf-b] during early neurogenesis. Development 1991;113:1193–206. [PubMed: 1811936]

Leger S, Brand M. Fgf8 and Fgf3 are required for zebrafish ear placode induction, maintenance and inner ear patterning. Mech Dev 2002;119:91–108. [PubMed: 12385757]

Litsiou A, Hanson S, Streit A. A balance of FGF, BMP and WNT signalling positions the future placode territory in the head. Development 2005;132:4051–62. [PubMed: 16093325]

Liu D, Chu H, Maves L, Yan YL, Morcos PA, Postlethwait JH, Westerfield M. Fgf3 and Fgf8 dependent and independent transcription factors are required for otic placode specification. Development 2003;130:2213–24. [PubMed: 12668634]

Luo T, Matsuo-Takasaki M, Lim JH, Sargent TD. Differential regulation of Dlx gene expression by a BMP morphogenetic gradient. Int J Dev Biol 2001;45:681–4. [PubMed: 11461005]

Matsuo-Takasaki M, Matsumura M, Sasai Y. An essential role of Xenopus Foxi1a for ventral specification of the cephalic ectoderm during gastrulation. Development 2005;132:3885–94. [PubMed: 16079156]

McLarren KW, Litsiou A, Streit A. DLX5 positions the neural crest and preplacode region at the border of the neural plate. Dev Biol 2003;259:34–47. [PubMed: 12812786]

Melby AE, Beach C, Mullins M, Kimelman D. Patterning the early zebrafish by the opposing actions of bozozok and vox/vent. Dev Biol 2000;224:275–85. [PubMed: 10926766]

Merlo GR, Paleari L, Mantero S, Zerega B, Adamska M, Rinkwitz S, Bober E, Levi G. The Dlx5 homeobox gene is essential for vestibular morphogenesis in the mouse embryo through a BMP4-mediated pathway. Dev Biol 2002;248:157–69. [PubMed: 12142028]

Meulemans D, Bronner-Fraser M. Gene-regulatory interactions in neural crest evolution and development. Dev Cell 2004;7:291–9. [PubMed: 15363405]

Miller-Bertoglio VE, Fisher S, Sanchez A, Mullins MC, Halpern ME. Differential regulation of chordin expression domains in mutant zebrafish. Dev Biol 1997;192:537–50. [PubMed: 9441687]

Moser M, Binder O, Wu Y, Aitsebaomo J, Ren R, Bode C, Bautch VL, Conlon FL, Patterson C. BMPER, a novel endothelial cell precursor-derived protein, antagonizes bone morphogenetic protein signaling and endothelial cell differentiation. Mol Cell Biol 2003;23:5664–79. [PubMed: 12897139]

Mullins MC, Hammerschmidt M, Kane DA, Odenthal J, Brand M, van Eeden FJ, Furutani-Seiki M, Granato M, Haffter P, Heisenberg CP, Jiang YJ, Kelsh RN, Nusslein-Volhard C. Genes establishing dorsoventral pattern formation in the zebrafish embryo: the ventral specifying genes. Development 1996;123:81–93. [PubMed: 9007231]

Nasevicius A, Ekker SC. Effective targeted gene ‘knockdown’ in zebrafish. Nat Genet 2000;26:216–20. [PubMed: 11017081]

Nguyen VH, Schmid B, Trout J, Connors SA, Ekker M, Mullins MC. Ventral and lateral regions of the zebrafish gastrula, including the neural crest progenitors, are established by a bmp2b/swirl pathway of genes. Dev Biol 1998;199:93–110. [PubMed: 9676195]

Nguyen VH, Trout J, Connors SA, Andermann P, Weinberg E, Mullins MC. Dorsal and intermediate neuronal cell types of the spinal cord are established by a BMP signaling pathway. Development 2000;127:1209–20. [PubMed: 10683174]

Nikaido M, Tada M, Saji T, Ueno N. Conservation of BMP signaling in zebrafish mesoderm patterning. Mech Dev 1997;61:75–88. [PubMed: 9076679]

Northcutt RG, Gans C. The genesis of neural crest and epidermal placodes: a reinterpretation of vertebrate origins. Q Rev Biol 1983;58:1–28. [PubMed: 6346380]

Ohyama T, Groves AK, Martin K. The first steps towards hearing: mechanisms of otic placode induction. Int J Dev Biol 2007;51:463–72. [PubMed: 17891709]

Park GT, Morasso MI. Bone morphogenetic protein-2 (BMP-2) transactivates Dlx3 through Smad1 and Smad4: alternative mode for Dlx3 induction in mouse keratinocytes. Nucleic Acids Res 2002;30:515–22. [PubMed: 11788714]

Pera E, Stein S, Kessel M. Ectodermal patterning in the avian embryo: epidermis versus neural plate. Development 1999;126:63–73. [PubMed: 9834186]

Pera EM, Ikeda A, Eivers E, De Robertis EM. Integration of IGF, FGF, and anti-BMP signals via Smad1 phosphorylation in neural induction. Genes Dev 2003;17:3023–8. [PubMed: 14701872]

Phillips BT, Bolding K, Riley BB. Zebrafish fgf3 and fgf8 encode redundant functions required for otic placode induction. Dev Biol 2001;235:351–65. [PubMed: 11437442]

Phillips BT, Kwon HJ, Melton C, Houghtaling P, Fritz A, Riley BB. Zebrafish msxB, msxC and msxE function together to refine the neural-nonneural border and regulate cranial placodes and neural crest development. Dev Biol 2006;294:376–90. [PubMed: 16631154]

Pizette S, Niswander L. BMPs negatively regulate structure and function of the limb apical ectodermal ridge. Development 1999;126:883–94. [PubMed: 9927590]

Poss KD, Shen J, Nechiporuk A, McMahon G, Thisse B, Thisse C, Keating MT. Roles for Fgf signaling during zebrafish fin regeneration. Dev Biol 2000;222:347–58. [PubMed: 10837124]

Pyati UJ, Webb AE, Kimelman D. Transgenic zebrafish reveal stage-specific roles for Bmp signaling in ventral and posterior mesoderm development. Development 2005;132:2333–43. [PubMed: 15829520]

Raible F, Brand M. Tight transcriptional control of the ETS domain factors Erm and Pea3 by Fgf signaling during early zebrafish development. Mech Dev 2001;107:105–17. [PubMed: 11520667]

Rajeevan MS, Ranamukhaarachchi DG, Vernon SD, Unger ER. Use of real-time quantitative PCR to validate the results of cDNA array and differential display PCR technologies. Methods 2001;25:443–51. [PubMed: 11846613]

Rentzsch F, Zhang J, Kramer C, Sebald W, Hammerschmidt M. Crossveinless 2 is an essential positive feedback regulator of Bmp signaling during zebrafish gastrulation. Development 2006;133:801–11. [PubMed: 16439480]

Riley BB. Genes controlling the development of the zebrafish inner ear and hair cells. Curr Top Dev Biol 2003;57:357–88. [PubMed: 14674487]

Riley BB, Phillips BT. Ringing in the new ear: resolution of cell interactions in otic development. Dev Biol 2003;261:289–312. [PubMed: 14499642]

Robledo RF, Lufkin T. Dlx5 and Dlx6 homeobox genes are required for specification of the mammalian vestibular apparatus. Genesis 2006;44:425–37. [PubMed: 16900517]

Robledo RF, Rajan L, Li X, Lufkin T. The Dlx5 and Dlx6 homeobox genes are essential for craniofacial, axial, and appendicular skeletal development. Genes Dev 2002;16:1089–101. [PubMed: 12000792]

Rossi CC, Hernandez-Lagunas L, Zhang C, Choi IF, Kwok L, Klymkowsky M, Artinger KB. Rohon-Beard sensory neurons are induced by BMP4 expressing non-neural ectoderm in Xenopus laevis. Dev Biol 2008;314:351–61. [PubMed: 18191829]

Sahly I, Andermann P, Petit C. The zebrafish eya1 gene and its expression pattern during embryogenesis. Dev Genes Evol 1999;209:399–410. [PubMed: 10370123]

Schlosser G. Induction and specification of cranial placodes. Dev Biol 2006;294:303–51. [PubMed: 16677629]

Scholpp S, Groth C, Lohs C, Lardelli M, Brand M. Zebrafish fgfr1 is a member of the fgf8 synexpression group and is required for fgf8 signalling at the midbrain-hindbrain boundary. Dev Genes Evol 2004;214:285–95. [PubMed: 15221377]

Serpe M, Umulis D, Ralston A, Chen J, Olson DJ, Avanesov A, Othmer H, O'Connor MB, Blair SS. The BMP-binding protein Crossveinless 2 is a short-range, concentration-dependent, biphasic modulator of BMP signaling in Drosophila. Dev Cell 2008;14:940–53. [PubMed: 18539121]

Shimizu T, Yamanaka Y, Nojima H, Yabe T, Hibi M, Hirano T. A novel repressor-type homeobox gene, ved, is involved in dharma/bozozok-mediated dorsal organizer formation in zebrafish. Mech Dev 2002;118:125–38. [PubMed: 12351176]

Sleptsova-Friedrich I, Li Y, Emelyanov A, Ekker M, Korzh V, Ge R. fgfr3 and regionalization of anterior neural tube in zebrafish. Mech Dev 2001;102:213–7. [PubMed: 11287195]

Solomon KS, Fritz A. Concerted action of two dlx paralogs in sensory placode formation. Development 2002;129:3127–36. [PubMed: 12070088]

Solomon KS, Kwak SJ, Fritz A. Genetic interactions underlying otic placode induction and formation. Dev Dyn 2004;230:419–33. [PubMed: 15188428]

Streit A. Extensive cell movements accompany formation of the otic placode. Dev Biol 2002;249:237–54. [PubMed: 12221004]

Suzuki A, Ueno N, Hemmati-Brivanlou A. Xenopus msx1 mediates epidermal induction and neural inhibition by BMP4. Development 1997;124:3037–44. [PubMed: 9272945]

Szeto DP, Kimelman D. Combinatorial gene regulation by Bmp and Wnt in zebrafish posterior mesoderm formation. Development 2004;131:3751–60. [PubMed: 15240553]

Thisse B, Thisse C, Weston JA. Novel FGF receptor (Z-FGFR4) is dynamically expressed in mesoderm and neurectoderm during early zebrafish embryogenesis. Dev Dyn 1995;203:377–91. [PubMed: 8589434]

Tribulo C, Aybar MJ, Nguyen VH, Mullins MC, Mayor R. Regulation of Msx genes by a Bmp gradient is essential for neural crest specification. Development 2003;130:6441–52. [PubMed: 14627721]

Whitlock KE, Westerfield M. The olfactory placodes of the zebrafish form by convergence of cellular fields at the edge of the neural plate. Development 2000;127:3645–53. [PubMed: 10934010]

Woda JM, Pastagia J, Mercola M, Artinger KB. Dlx proteins position the neural plate border and determine adjacent cell fates. Development 2003;130:331–42. [PubMed: 12466200]

Yamamoto Y, Oelgeschlager M. Regulation of bone morphogenetic proteins in early embryonic development. Naturwissenschaften 2004;91:519–34. [PubMed: 15517134]

Yang L, Zhang H, Hu G, Wang H, Abate-Shen C, Shen MM. An early phase of embryonic Dlx5 expression defines the rostral boundary of the neural plate. J Neurosci 1998;18:8322–30. [PubMed: 9763476]

Zhang JL, Huang Y, Qiu LY, Nickel J, Sebald W. von Willebrand factor type C domain-containing proteins regulate bone morphogenetic protein signaling through different recognition mechanisms. J Biol Chem 2007;282:20002–14. [PubMed: 17483092]

Zhang JL, Qiu LY, Kotzsch A, Weidauer S, Patterson L, Hammerschmidt M, Sebald W, Mueller TD. Crystal structure analysis reveals how the Chordin family member crossveinless 2 blocks BMP-2 receptor binding. Dev Cell 2008;14:739–50. [PubMed: 18477456]

Zuniga A, Haramis AP, McMahon AP, Zeller R. Signal relay by BMP antagonism controls the SHH/FGF4 feedback loop in vertebrate limb buds. Nature 1999;401:598–602. [PubMed: 10524628]

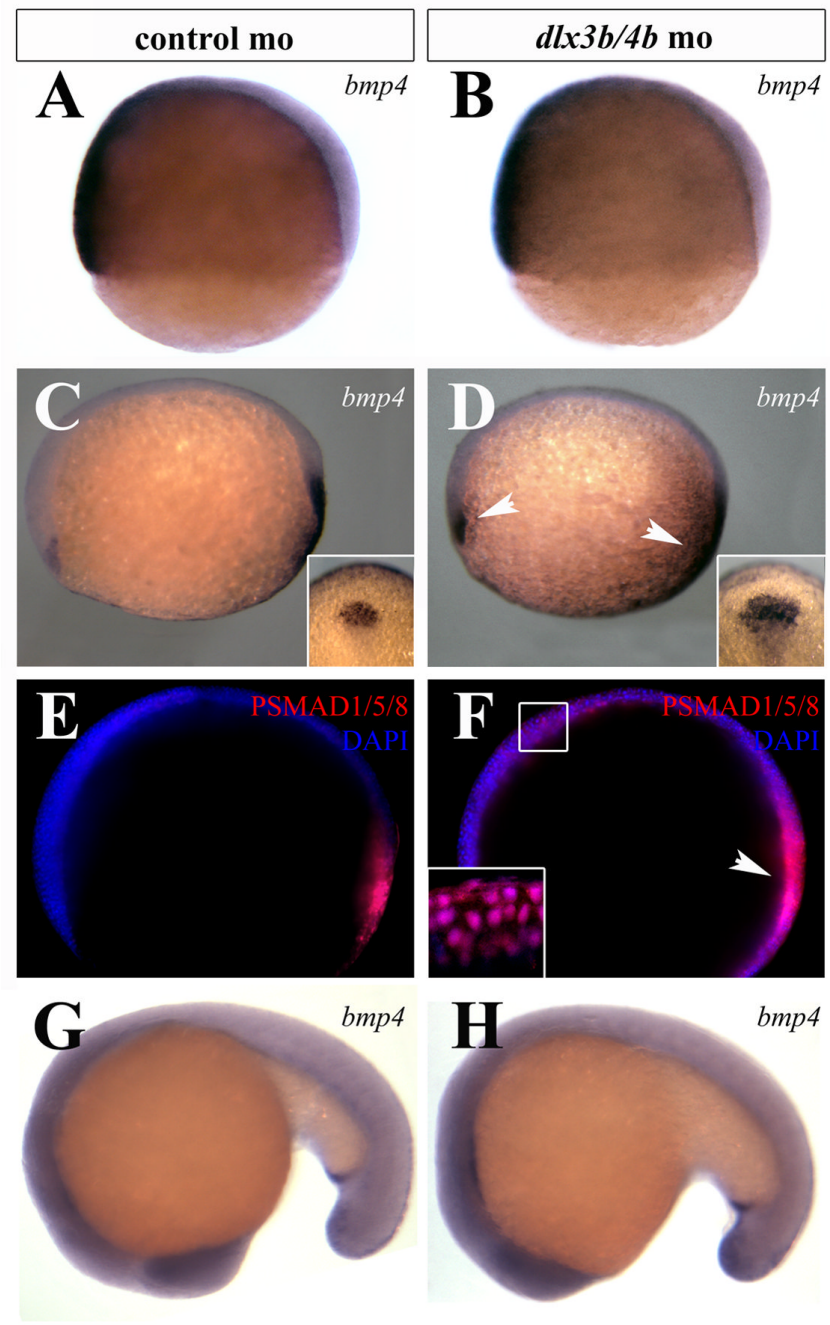

Figure 1.

BMP activity is transiently increased during early somitogenesis in Dlx3b/4b morphants. (A,B) *bmp4* expression is unaffected in Dlx3b/4b morphants prior to the onset of *dlx3b/4b* expression in 70% epiboly embryos. (C,D) At bud stage, the domain of *bmp4* expression is expanded in the prechordal plate and tailbud of Dlx3b/4b morphants (D). Insets depict the increase of the prechordal domain. (E,F) Antibodies against PSMAD1/5/8 (red) reveal an increase in cells responding to BMP activity of Dlx3b/4b morphants (F). DAPI-stained nuclei are blue. Inset in (F) is a high magnification image depicting PSMAD1/5/8 co-localization with DAPI-stained nuclei. (G,H) *bmp4* expression in Dlx3b/4b morphants is comparable to controls at 18-somites.

All views are lateral views, with ventral to the left in (A,B), anterior to the left in (C-F), and anterior to the bottom in (G,H). Insets in (C,D) are dorsal views, with anterior to the top.

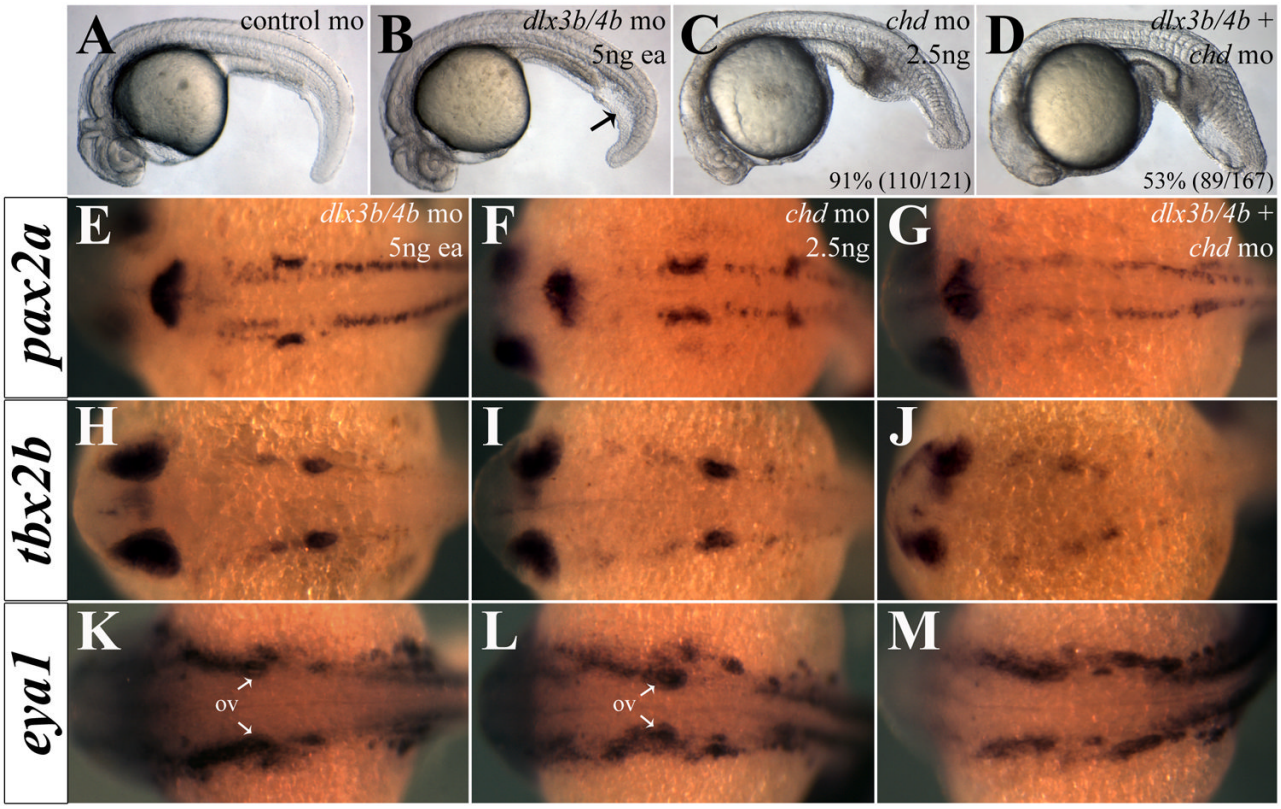

Figure 2.

Depletion of Chd reveals anti-BMP function of Dlx3b/4b. (A-D) Intermediate cell mass of the tail is increased in Dlx3b/4b morphants (B), reminiscent of a ventralization phenotype. Injection of a low dose of *chd*-mo results in a mild V1 ventralization phenotype (C). Knockdown of Chd and Dlx3b/4b increases the severity of ventralization (D). (E-M) Heightened BMP activity in Chd/Dlx3b/4b triple morphant embryos severely reduces otic expression of *eya1* (E-G), *pax2a* (H-J), and *tbx2b* (K-M), while leaving expression in surrounding tissue intact. (A-D) are lateral views and (E-M) are dorsal views, with anterior to the left. All embryos are 24hpf.

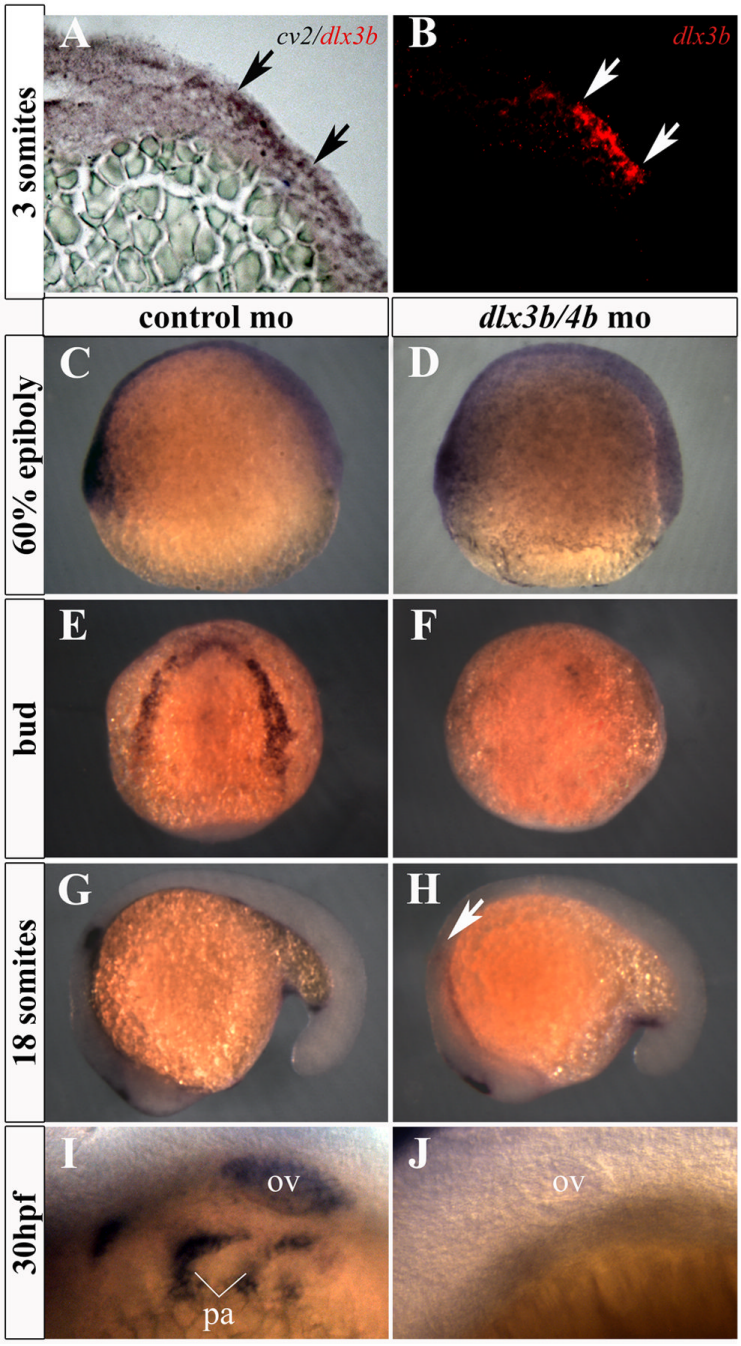

Figure 3.

cv2 expression is lost from the PPR, otic placode, and pharyngeal arches in Dlx3b/4b morphants. (A,B) *cv2* (purple) is co-expressed with *dlx3b* (red) in the ectoderm of the PPR. Transverse sections were taken through the neural plate of 3-somite embryos. (C,D) Prior to the onset of *dlx3b/4b* expression, *cv2* expression is unaffected on the ventral side of 60% epiboly embryos. (E,F) *cv2* expression is lost from the PPR in Dlx3b/4b morphants (F). (G,H) *cv2* expression is lost from the otic placode in 18 somite Dlx3b/4b morphants (H). (I,J) *cv2* expression is lost from the otic vesicle and pharyngeal arches in 30hpf (hours post fertilization) embryos (J). ov, otic vesicle; pa, pharyngeal arches. All views are lateral except (E,F), which are dorsal views.

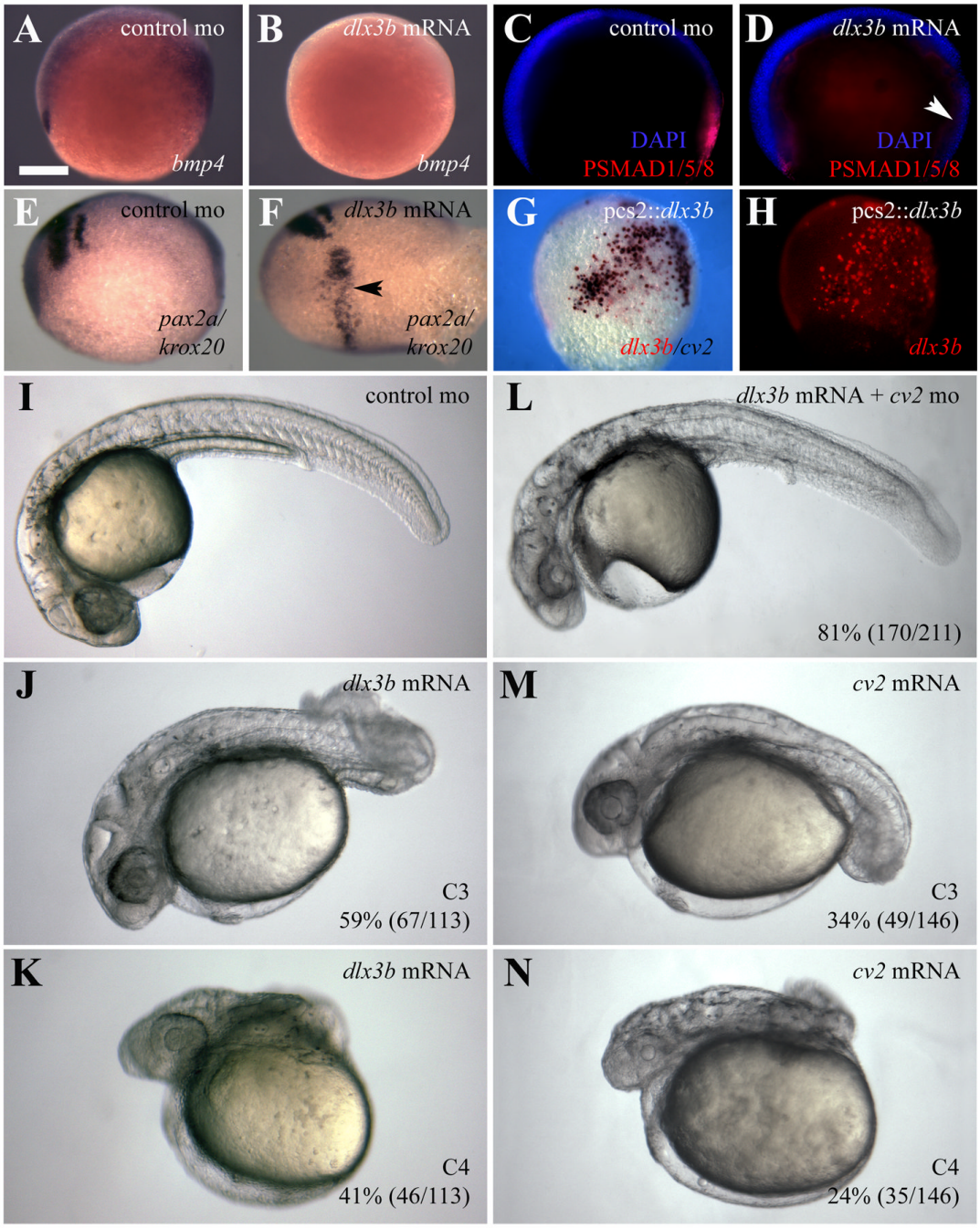

Figure 4.

dlx3b overexpression dorsalizes the zebrafish embryo. (A-D) Embryos ectopically expressing *dlx3b* mRNA display molecular read-outs consistent with reduced BMP activity. (A,B) *bmp4* expression is reduced from the prechordal plate and tailbud of embryos ectopically expressing *dlx3b* (B). (C,D) Antibodies against PSMAD1/5/8 (red) reveal that BMP activity is reduced in embryos ectopically expressing *dlx3b* mRNA (D). (E,F) Riboprobes against *krox20* and *pax2a* reveal a widening of the hindbrain in embryos ectopically expressing *dlx3b* mRNA (F). (G,H) Ectopic *dlx3b* DNA (red) can induce ectopic *cv2* expression (purple). (I-N) Ectopic expression of *dlx3b* mRNA resembles the dorsalization seen in embryos ectopically expressing *cv2*. Knockdown of Cv2 can rescue the dorsalization seen in 81%

(170/211) of embryos ectopically expressing *dlx3b* mRNA (L). (I-N) 30hpf embryos; lateral views, with anterior to the left. Embryos were grouped into dorsalization categories based on previous classifications (Kishimoto et al., 1997; Mullins et al., 1996). (A-F) Bud stage embryos. Lateral views, with anterior to the left. (G,H) 80% epiboly embryos; lateral views, with ventral to the left.

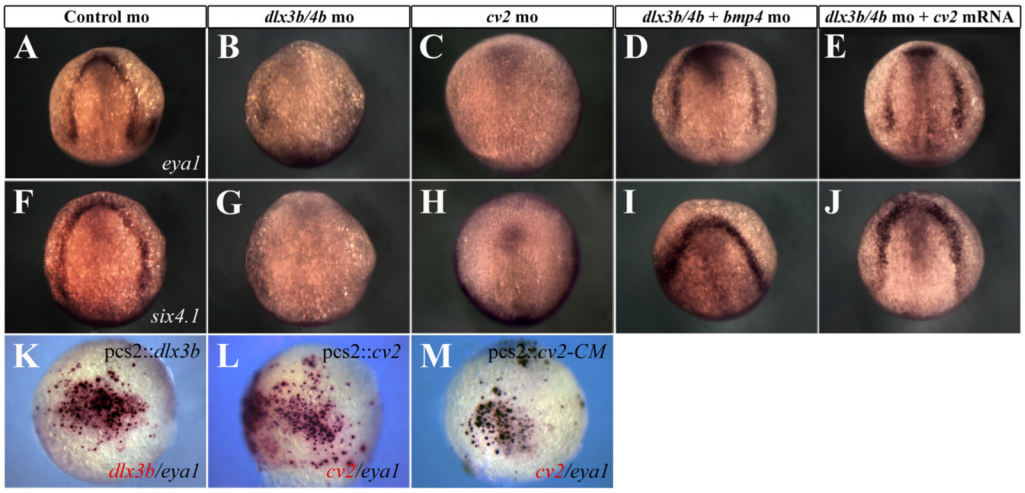

Figure 5.

dlx3b/4b and *cv2* are required for PPR marker expression. (A-J) *eya1* (A-E) and *six4.1* (F-J) expression are reduced in the PPR of Dlx3b/4b (B,G) and Cv2 (C,H) morphants, but can be rescued when Bmp4 is knocked down (D,I) or when *cv2* mRNA is ectopically expressed (E,J). (K,L) Ectopic *dlx3b* or *cv2* (red) can induce ectopic *eya1* (purple). (M) All cells ectopically expressing the uncleavable form of Cv2, *cv2-CM* (red), ectopically express *eya1* (purple). (A-J) Bud stage embryos; dorsal views, with anterior to the top. (K-M) 80% epiboly embryos; lateral views, with ventral to the left.

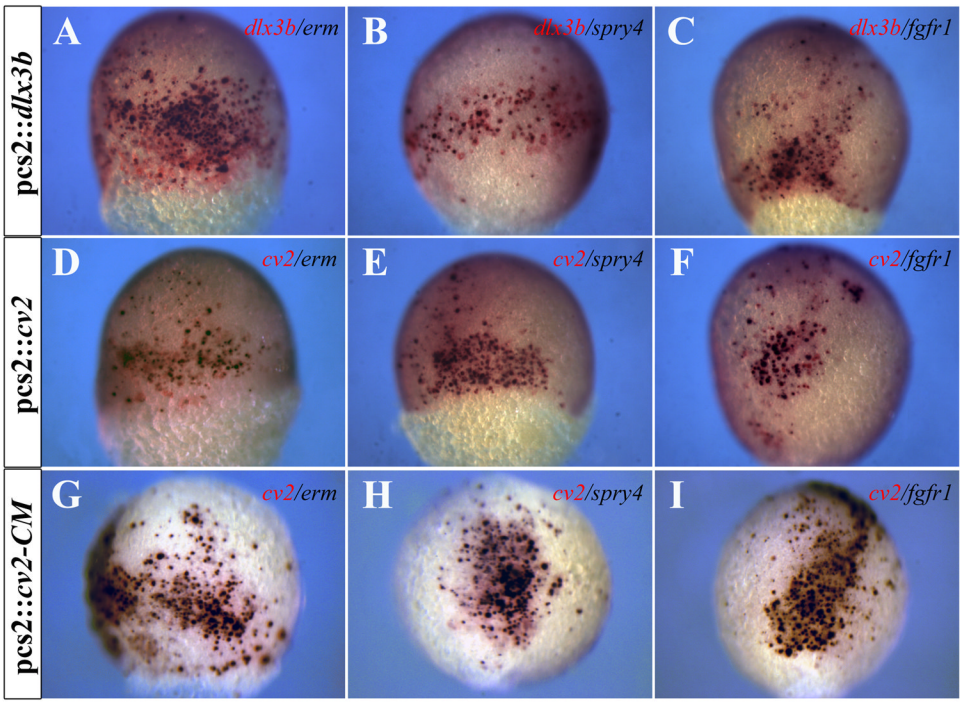

Figure 6.
Ectopic *dlx3b* or *cv2* expression can induce ectopic FGF activity. (A-C) Ectopic *dlx3b* expression (red) can induce ectopic expression of *erm*, *spry4*, and *fgfr1* (purple). (D-F) Ectopic *cv2* expression (red) can induce ectopic expression of *erm*, *spry4*, and *fgfr1* (purple). (G-I) All cells ectopically expressing the uncleavable form of Cv2, *cv2-CM* (red), ectopically express *erm*, *spry4*, and *fgfr1* (purple). (A-I) 80% epiboly embryos; lateral views.

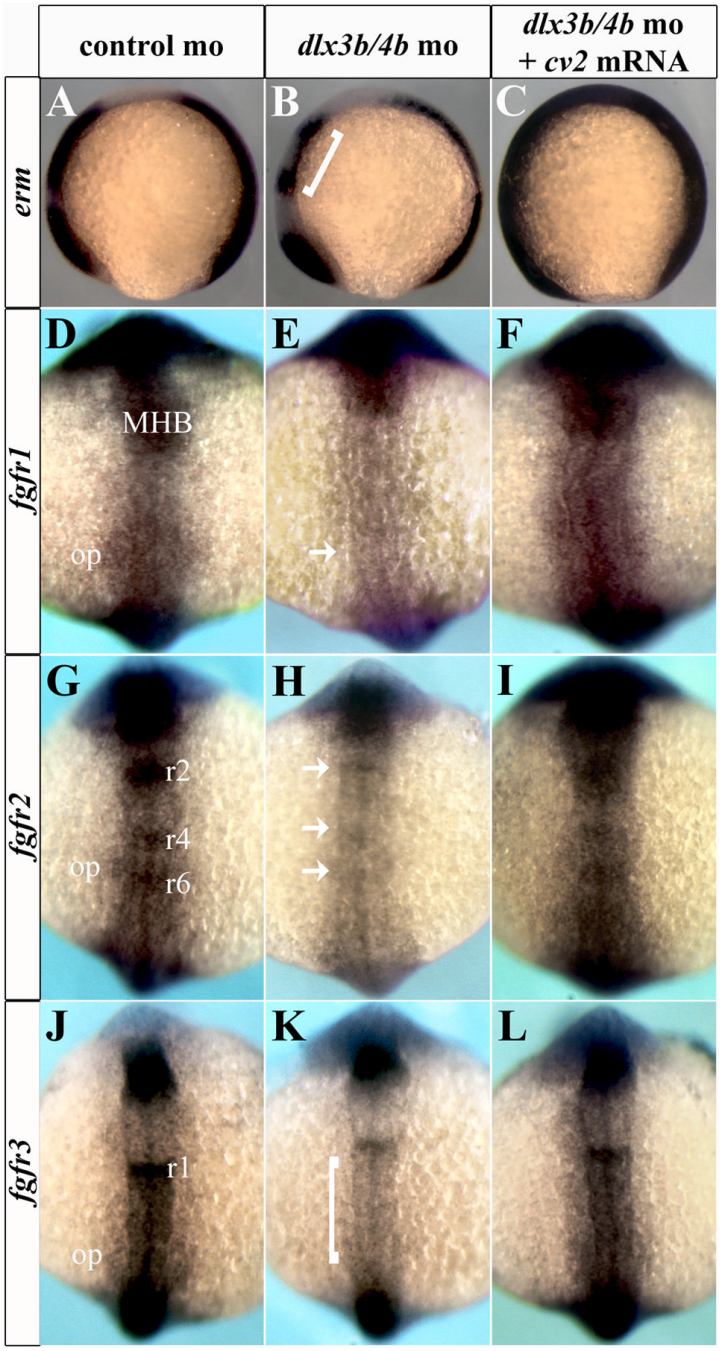

Figure 7.

fgfr expression is lost from the otic placode and hindbrain of Dlx3b/4b morphants. *erm* and *fgfr1-3* expression are lost from the otic placode and hindbrain of Dlx3b/4b morphants (B,E,H,K). Brackets in (B,K) depict reduction of *erm* (B) and *fgfr3* (K) staining in the hindbrain. Arrows in (E,H) depict loss of *fgfr1* staining (E) from the otic placode and loss of *fgfr2* staining (H) from the hindbrain of Dlx3b/4b morphants. *erm* and *fgfr1-3* expression can be restored to the otic placode and hindbrain when *cv2* mRNA is ectopically expressed in Dlx3b/4b morphants (C,F,I,L). (A-P) 6 somite embryos; dorsal view with anterior to the top. MHB, midbrain-hindbrain boundary; r1, rhombomere 1; r2, rhombomere 2; r3, rhombomere 3; r4, rhombomere 4; r6, rhombomere 6; op, otic placode.

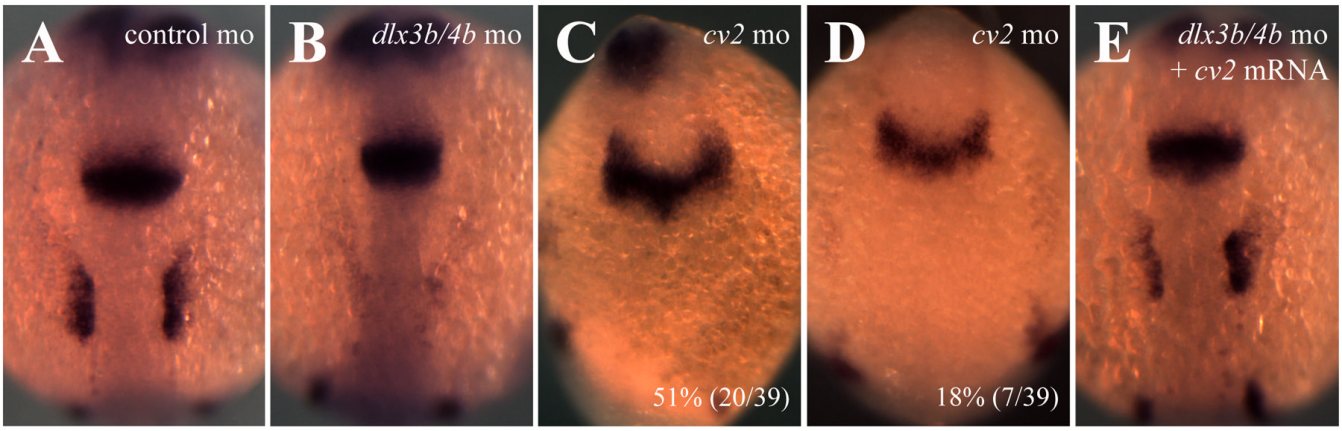

Figure 8.

pax2a expression in the otic placode requires Cv2. (A-E) *pax2a* expression is lost from the otic placode of Dlx3b/4b (B) and in 69% (27/39) of Cv2 (C,D) morphants. *pax2a* expression can be restored to the otic placode when *cv2* mRNA is ectopically expressed in Dlx3b/4b morphants (E). (A-E) 6-somite embryos; dorsal view, with anterior to the top.

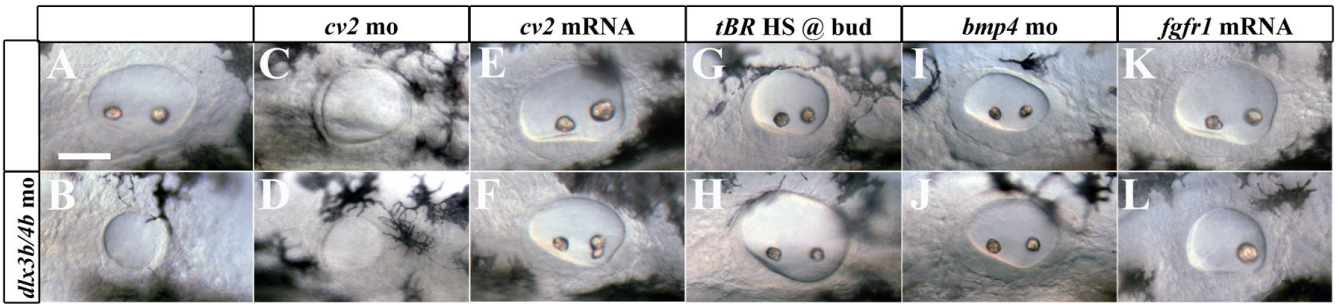

Figure 9.

Manipulation of PPR-inducing signals can rescue the otic phenotype of Dlx3b/4b morphants. (B) Dlx3b/4b morphants display a small, circular otic vesicle that lacks otoliths. (C,D) The otic phenotype of Cv2 morphants resembles that of Dlx3b/4b morphants (B), and is not significantly affected by the additional loss of Dlx3b/4b (D). (E,F) Ectopic expression of *cv2* mRNA can rescue the Dlx3b/4b otic phenotype (F). (G-L) While heat shock of *tBR* embryos (G), knockdown of Bmp4 (I), or ectopic *fgfr1* expression (K) does not affect ear morphology, each is able to partially rescue the otic phenotype of Dlx3b/4b morphants (H,J,L). All embryos are 30hpf; lateral views, with anterior to the left.